Spectral function for a conducting sheet containing circular inclusions

B. R. Djordjević, J. H. Hetherington, and M. F. Thorpe
Department of Physics and Astronomy and Center for Fundamental Materials Research, Michigan State University, East Lansing, Michigan 48824
(Received 15 January 1996)

The conductivity (or dielectric behavior) of a binary composite system is conveniently expressed in terms of a *spectral function*, which is determined by the geometry of the composite. In this paper we examine the case of circular inclusions in a conducting sheet and keep terms up to second order in the inclusion concentration f. The two-inclusion problem can be solved exactly using multiple images, and we use this solution to construct the spectral function. We show that the spectral function is a truncated Lorentzian that can be calculated in a simple closed form. Both the weight and the width of the spectral function are linear in f. [S0163-1829(96)05022-9]

I. INTRODUCTION

Exact results for the properties of composite materials are rare, and so the few that exist are particularly important as aids to our understanding. Although spectral functions are widely used in physics, their use in composite materials has not been widespread. This is mainly because this attractive formalism is difficult to apply to particular composite geometries, because of the numerical difficulty of computing the spectral function. In this paper we examine a nontrivial example of a spectral function that can be calculated exactly. This example involves the calculation of the spectral function of a sheet containing circular inclusions with a different conductivity from that of the host. Using the well-known technique of multiple dipole images, the terms in the effective conductivity up to second order in the concentration of inclusions f can be found. We have been able to express the spectral function in a rapidly convergent series. We show that the spectral function is a truncated Lorentzian with weight f and a width that is proportional to f, and we are able to give the final result in a very simple form.

It has been shown by Bergman,[1] Milton,[2,3] and Golden Papanicolau[4] that for any two-phase composite medium, which on average is uniform and isotropic, the effective conductivity σ (or dielectric constant) can be written as

$$\frac{\sigma}{\sigma_0}=1-\int_0^1\frac{g(u)du}{t-u} \tag{1}$$

where

$$t=\frac{\sigma_0}{\sigma_0-\sigma_1}. \tag{2}$$

σ_0 and σ_1 are the conductivities of the host and the inclusions, respectively, and $g(u)$ is the *spectral function*. The spectral function is fully determined by the geometry of the two-phase medium, and does not depend upon the material parameters σ_0 and σ_1. It is therefore a purely geometric quantity. It provides a very compact way of giving the information to calculate via a single integral (1) the conductivity of a series of composites with different material parameters, but the same geometry. It is particularly useful in a given composite when the conductivities σ_0 and σ_1 are frequency dependent (and hence complex). In this case the effective conductivity σ is also complex, of course.

The spectral function $g(u)$ can be used in any dimension $\mathscr{d}$ and for any volume fraction f of inclusions. Indeed, the decision as to what constitutes the matrix and what is the inclusion is arbitrary, although in the dilute limit we will of course make the circular objects the inclusions. The spectral function $g(u)$ can be shown to have the following properties.[1,5]

(1) It is a real positive definite function for $0<u<1$ and zero outside this range.

(2) The total weight and the first integral are given by

$$\int_0^1 g(u)du=f, \tag{3}$$

$$\int_0^1 ug(u)du=\frac{f(1-f)}{\mathscr{d}}, \tag{4}$$

where f is concentration (volume fraction) of the phase σ_1 in the host of σ_0, and $\mathscr{d}$ is the dimension. This can be obtained using the weak-scattering limit.[6] It is convenient sometimes to define the normalized moments $\langle u^n\rangle$ of the spectral function by

$$\langle u^n\rangle=\frac{\int_0^1 u^n g(u)du}{\int_0^1 g(u)du} \tag{5}$$

so that from (4) we have

$$\langle u\rangle=\frac{(1-f)}{\mathscr{d}}. \tag{6}$$

The higher-order moments depend on the details, and are not known *a priori*. In this paper we will apply this formalism to a two-dimensional sheet containing circular inclusions, and obtain the spectral function to second order in the area fraction f of inclusions. The layout of the paper is as follows. In the next section we restrict the form of the conductivity σ by using the reciprocity theorem that is valid in two dimensions

 © 1996 The American Physical Society

(2D). In Sec. III, we use the method of multiple images to write down the position and strengths of the dipoles in a pair of circular inclusions. In Sec. IV, we examine the results in more detail, particularly for the case of perfectly conducting inclusions. In Sec. V, we obtain the effective conductivity by averaging over the dipole moments of the pairs that we have found previously. This solution is then rearranged into a form from which the spectral function can be derived in Secs. VI and VII. Finally, in the conclusions, we discuss the uses of this kind of approach.

II. GENERAL FORM FOR THE TWO-DIMENSIONAL CONDUCTIVITY

The problem of circular and polygonal holes in a two-dimensional conducting sheet was recently investigated by Thorpe[7] up to the first order in the area fraction of inclusions, using the conformal mapping technique. From the other side, the general problem for circular inclusions had been solved earlier up to the second order by Peterson and Hermans[8] using bipolar coordinates.

In this paper we use the method of electrical images to solve the problem of the effective conductivity in the conducting sheet containing circular inclusions of an arbitrary conductivity. This method is not limited to holes and perfectly conducting inclusions, as is the conformal mapping technique.

We first consider one isolated pair of identical circles with radius a separated by a distance R. Considering the two independent cases of parallel and perpendicular external electric field, we construct the infinite set of dipole, or doublet images.[9] Each dipole image is found in a simple continued-fraction form. We find and solve the appropriate difference equation for successive dipole images to get all dipole moment images, now in closed form, in terms of hyperbolic functions. All further calculations are based on these dipole images. Naturally, the total dipole moment of the two circles is given by the sum of all image-dipole moments in the case of parallel external field, and by the same sum, but with alternating signs in the case of perpendicular external field.

The reciprocity theorem[10,11] for the two-phase medium in 2D states that the following relation must hold:[12]

$$\sigma(\sigma_0,\sigma_1)\sigma'(\sigma_1,\sigma_0)=\sigma_0\sigma_1, \tag{7}$$

where σ_0 and σ_1 are the conductivities of the two phases, and $\sigma(\sigma_0,\sigma_1)$ and $\sigma'(\sigma_1,\sigma_0)$ are the effective conductivities of the original system and the one with the same geometry but σ_0 and σ_1 interchanged.

We find the generalization of the effective conductivity[12] to the second order in the concentration f of the inclusion phase 1 in the host phase 0. The effective conductivity then must be of the form

$$\frac{\sigma}{\sigma_0}=1+f\gamma G(\gamma)+f^2H(\gamma)+O(f^3), \tag{8}$$

where

$$\gamma=\frac{\sigma_1-\sigma_0}{\sigma_1+\sigma_0} \tag{9}$$

and the function $G(\gamma)$ is an *even* function of γ (Ref. 12) as follows from the reciprocity theorem (7). Similarly, for interchanged phases 0 and 1 ($\gamma\Rightarrow-\gamma$), the effective conductivity σ' is given as

$$\frac{\sigma'}{\sigma_1}=1-f\gamma G(\gamma)+f^2H(-\gamma)+O(f^3). \tag{10}$$

Multiplying (8) by (10) and using the reciprocity theorem (7), we get the second order in concentration f

$$H(\gamma)+H(-\gamma)-\gamma^2G^2(\gamma)=0, \tag{11}$$

from which it is clear that the function $H(\gamma)$ must generally be of the form

$$H(\gamma)=\tfrac{1}{2}\gamma^2G^2(\gamma)+\gamma L(\gamma) \tag{12}$$

where the function $L(\gamma)$ is an *even* function of γ.

The weak-scattering limit[12] gives $L(\gamma)=\gamma F(\gamma)$, where $F(\gamma)$ is an *odd* function of γ (proportional to γ for small γ), and $F(0)$ is zero. So, finally, (8) becomes

$$\frac{\sigma}{\sigma_0}=1+f\gamma G(\gamma)+\tfrac{1}{2}f^2\gamma^2G^2(\gamma)+f^2\gamma^2F(\gamma)+O(f^3), \tag{13}$$

where $G(\gamma)$ and $F(\gamma)$ are an even and an odd function of γ, respectively. The area fraction f can be written as

$$f=n\pi a^2, \tag{14}$$

where n is the number of inclusions per unit area, each with area πa^2. Two usual limits are obtained when the inclusion is a hole ($\gamma=-1$) and when the inclusion is perfectly conducting ($\gamma=1$). Equation (13) is valid generally but for circular inclusions $G(\gamma)=2$.[7] So for circles as inclusions (13) simplifies to

$$\frac{\sigma}{\sigma_0}=1+2\gamma f+2\gamma^2f^2+\gamma^2f^2F(\gamma)+O(f^3) \tag{15}$$

and our goal is to calculate the function $F(\gamma)$ which contains the pair terms in the effective conductivity.

We relate the function $F(\gamma)$ to the pair contribution to the polarizability $\Delta\beta$. This is defined as the mean change in the polarizability of a single inclusion due to the presence of the other inclusions. To leading order, $\Delta\beta$ can be obtained from the dipole moment of pairs. Indeed, we have stressed in previous papers[7,12] that the conductivity of a sample is directly related to the dipole moment of *all* the inclusions. Once we have all dipole moment images in the aligned and perpendicular external field, it is straightforward to find the polarizability change $\Delta\beta$ be averaging the parallel and perpendicular two-circle total dipole moments and integrating over the whole sheet. Then we use the relation

$$\gamma^2f^2F(\gamma)=n\Delta\beta. \tag{16}$$

III. DIPOLE MOMENTS

We shall first consider the case of an aligned (parallel) external electric field with respect to the line connecting the centers of the two circles, as shown in Fig. 1. The circles are

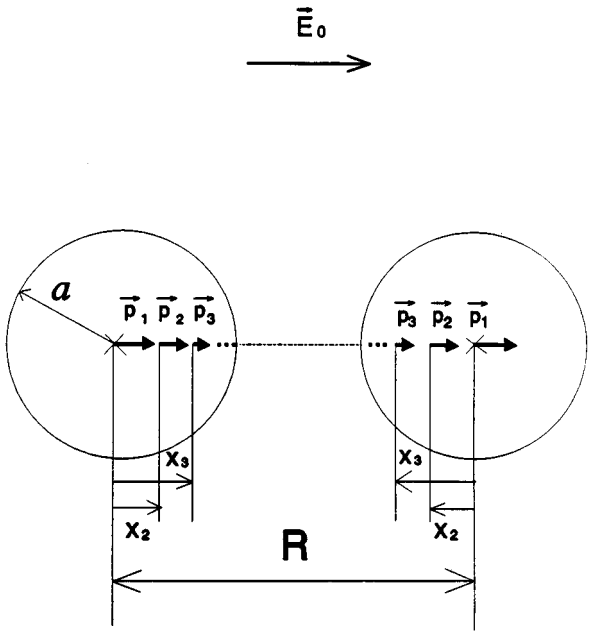

FIG. 1. Orientation of the dipole images for two circles in a parallel applied field E_0, showing the notation in the text.

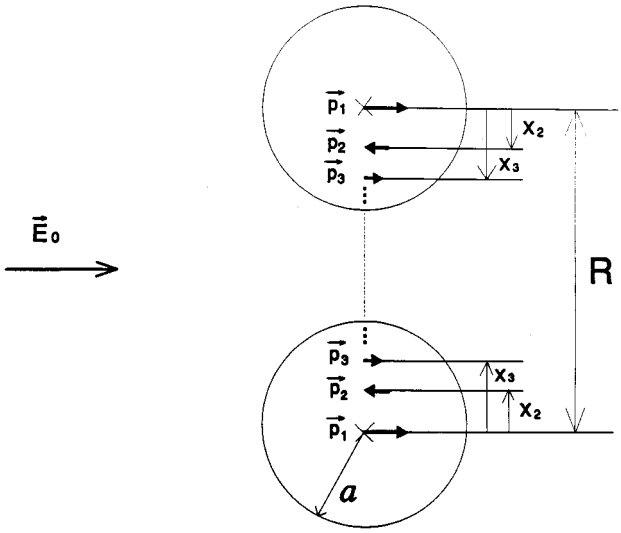

FIG. 2. Orientation of the dipole images for two circles in a perpendicular applied field E_0, showing the notation in the text.

not charged and have an arbitrary conductivity σ_1. In the external field they become polarized, i.e., there is an induced dipole moment on each circle. So it is intuitively clear that we have to deal with dipoles in constructing the infinite set of images which solves this electrostatic problem.

The images of a dipole can be derived from the combination of the separate images of the pair of charges forming the dipole.[9] By definition, a two-dimensional dipole is a combination of a positive line charge and a negative line charge, an infinitesimal distance apart, so arranged that the product of charge and distance remains finite.

One circle in a uniform external field is completely described by one dipole at the center of the circle. We start from that dipole at the center of one circle which we denote by p_1, given by

$$p_1 = 2\pi\gamma E_0 a^2. \tag{17}$$

Assuming that we started from the circle to the right, and taking in account the presence of the other circle to the left, we find the dipole image p_2 of p_1 in the circle to the left. Now we find the next dipole image p_3 of p_2 in the circle to the right. Continuing in that way we construct an infinite set of dipole images. Odd-numbered images are all inside the right circle, and all even-numbered images are inside the left circle. But, due to the symmetry between the two circles, there must be another infinite set of images generated by placing the first dipole p_1 at the center of the left circle. The complete solution of the problem consists of two infinite sets of images, redistributed in such a way that each circle now has the same infinite set of images $p_1, p_2, p_3, \ldots$, which are given in the simple, continued-fraction form

$$p_2 = \gamma\left(\frac{a}{R}\right)^2 p_1,$$

$$p_3 = \gamma\left(\frac{a}{R-\dfrac{a^2}{R}}\right)^2 p_2, \tag{18}$$

$$p_4 = \gamma\left(\frac{a}{R-\dfrac{a^2}{R-\dfrac{a^2}{R}}}\right)^2 p_3,$$

$$\vdots$$

where γ is given by (9), a is the radius of each circle, R is the separation between their centers, and p_1 is given by (17). All images of dipole moments have the same direction, along the applied field, as shown in Fig. 1.

The case of the perpendicular external field is shown in Fig. 2. Due to the direction of the applied field, all dipole moments are now perpendicular to the horizontal connecting the centers of the two circles. The first dipole image p_2 now has the opposite direction with respect to the initial dipole p_1. The alternating directions of successive images are the only new thing here, so we can repeat essentially the same procedure we used for the parallel field case, to get exactly the same infinite set of dipole images whose magnitudes are given by (17) and (18), as before. The alternating orientations of these dipoles are represented symbolically in Fig. 2.

The positions of the first few images in both circles, measured from their respective centers, as shown in Figs. 1 and 2, are found in a similar continued-fraction form:

$$x_1=0,$$

$$x_2=\frac{a^2}{R},$$

$$x_3=\frac{a^2}{R-\frac{a^2}{R}}, \tag{19}$$

$$x_4=\frac{a^2}{R-\frac{a^2}{R-\frac{a^2}{R}}},$$

. . .

These positions hold for both the parallel and perpendicular cases.

Combining (17)–(19), it is easy to see that the dipole moments satisfy the difference equation

$$\frac{1}{\sqrt{p_{s+1}}}+\frac{1}{\gamma\sqrt{p_{s+1}}}=\frac{R}{a}\frac{1}{\sqrt{\gamma p_s}}. \tag{20}$$

Solution of (20) gives all dipole images in terms of hyperbolic functions,

$$p_s=2\pi E_0 a^2\gamma^s\left(\frac{\sinh\alpha}{\sinh s\alpha}\right)^2 \tag{21}$$

where α is given by the relation

$$\cosh\alpha=\frac{R}{2a}. \tag{22}$$

(21) is our main result for dipole moment images, and all further calculations are based on it.

It is conceptually obvious that in the parallel field the total dipole moment is given by the sum of all dipole images multiplied by a factor of 2 (two circles):

$$P_\parallel=2\sum_{s=1}^{\infty} p_s. \tag{23}$$

Using (21) we get

$$P_\parallel=4\pi E_0 a^2\sum_{s=1}^{\infty}\gamma^s\left(\frac{\sinh\alpha}{\sinh s\alpha}\right)^2, \tag{24}$$

which is the total dipole moment of two circles in the parallel external field.

In a perpendicular external field, the only difference is the alternating orientation of the consecutive dipole moments, while they still have the same magnitudes as in the parallel field case. So the total dipole moment of two circles becomes

$$P_\perp=4\pi E_0 a^2\sum_{s=1}^{\infty}(-1)^{s+1}\gamma^s\left(\frac{\sinh\alpha}{\sinh s\alpha}\right)^2. \tag{25}$$

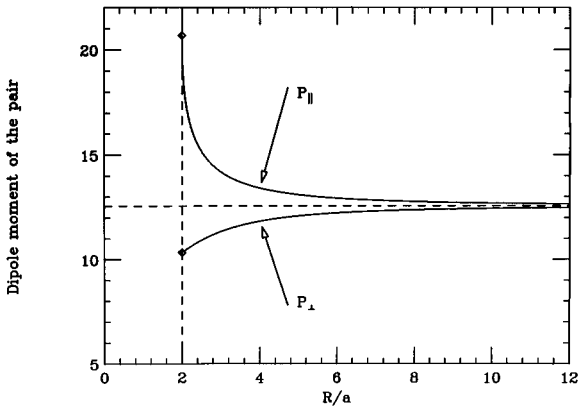

FIG. 3. Total dipole moment $P_\parallel$ and $P_\perp$ of two perfectly conducting circles in parallel and perpendicular external fields. The two diamond symbols when the circles touch at $R/a=2$ are from Eqs. (28) and (29).

IV. PERFECTLY CONDUCTING INCLUSIONS

As an interesting sideline, we look at some properties of a single pair of inclusions. The formulas for this case have a particularly simple form. We calculate the total dipole moment of the two perfectly conducting ($\gamma=1$) circular inclusions in an external field, separated by distance R.

Using (24) with $\gamma=1$ we have for perfectly conducting circles

$$P_\parallel=4\pi E_0 a^2\sum_{s=1}^{\infty}\left(\frac{\sinh\alpha}{\sinh s\alpha}\right)^2, \tag{26}$$

which is the total dipole moment of two perfectly conducting circles in the parallel external field.

In a perpendicular external field, using (25) with $\gamma=1$, we get

$$P_\perp=4\pi E_0 a^2\sum_{s=1}^{\infty}(-1)^{s+1}\left(\frac{\sinh\alpha}{\sinh s\alpha}\right)^2. \tag{27}$$

Using (26) and (27), we numerically calculate the total dipole moment dependence on the separation R/a of the two circular inclusions, in both cases. These graphs are shown in Fig. 3. When the circles touch, (26), and (27) give exact values for the two dipole moments (with $\alpha\to 0$):

$$P_\parallel=4\pi E_0 a^2\sum_{s=1}^{\infty}\frac{1}{s^2}=4\pi E_0 a^2\zeta(2)=\frac{2}{3}E_0 a^2\pi^3, \tag{28}$$

$$P_\perp=4\pi E_0 a^2\sum_{s=1}^{\infty}(-1)^{s+1}\frac{1}{s^2}=2\pi E_0 a^2\zeta(2)=\frac{1}{3}E_0 a^2\pi^3, \tag{29}$$

where the sums are expressed in terms of the Riemann ζ function.[13]

In this particular case of perfectly conducting circular inclusions, and in parallel external field, each consecutive dipole image introduces some change of the potential on each circle. The first few contributions in the decreasing potential of the circle O_1, which correspond to the first few dipole images $p_1, p_2, p_3, \ldots$, are

$$V_1 = 0,$$

$$V_2 = -\frac{1}{2\pi}\frac{p_1}{R},$$

$$V_3 = -\frac{1}{2\pi}\frac{p_2}{R-\frac{a^2}{R}}, \tag{30}$$

$$V_4 = \frac{1}{2\pi}\frac{p_3}{R-\frac{a^2}{R-\frac{a^2}{R}}},$$

.
.
.

where $p_1, p_2, p_3, \ldots$ are given by (17) and (18). In general,

$$V_s = \frac{x_s p_{s-1}}{2\pi a^2}. \tag{31}$$

In the absence of inclusions, the external electric field E_0 creates a potential difference between the two centers given by

$$\Delta V_E = E_0 R. \tag{32}$$

The total potential difference, i.e., the voltage ΔV, between the two perfectly conducting circles in the external field is given by

$$\Delta V = \Delta V_E = 2\sum_{s=2}^{\infty} |V_s|. \tag{33}$$

Combining (18), (19), and (30) the total voltage can be expressed in terms of a sum over hyperbolic functions,

$$\Delta V = E_0 a\left(\frac{R}{a} - 2\sum_{s=2}^{\infty}\frac{(\sinh\alpha)^2}{\sinh s\alpha \sinh(s-1)\alpha}\right). \tag{34}$$

The series in (34) is summable to a simple form. To show this, rewrite this sum with the help of (22) and in terms of the new variable $y = e^{\alpha}$. (34) then becomes

$$\Delta V = E_0 a\left[y + \frac{1}{y} - 2\left(y - \frac{1}{y}\right)^2 \times \sum_{s=2}^{\infty}\frac{1}{(y^s - y^{-s})(y^{s-1} - y^{-(s-1)})}\right]. \tag{35}$$

Rewriting in terms of partial fractions (35) becomes

$$\Delta V = E_0 a\left[y + \frac{1}{y} + 2\left(y - \frac{1}{y}\right)\sum_{s=2}^{\infty}\left(\frac{1}{y^{2s}-1} - \frac{1}{y^{2s-2}-1}\right)\right]. \tag{36}$$

Writing explicitly the first few terms in the sum, it is easy to see that only one term in the second partial fraction survives for $s=2$, while all others cancel each other to give

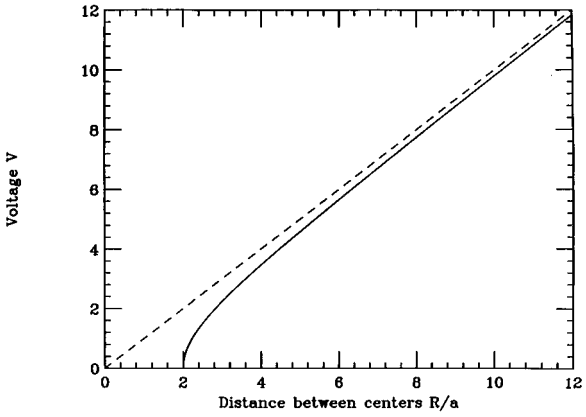

FIG. 4. Voltage between the two perfectly conducting circles in the external field is shown as a solid line. The dashed line would be the voltage in the absence of the conducting circles (i.e., just host material).

$$\Delta V = E_0 a\left(y - \frac{1}{y}\right) \tag{37}$$

and hence

$$\Delta V = E_0\sqrt{R^2 - 4a^2}. \tag{38}$$

This remarkably simple result for the voltage between two perfectly conducting circular inclusions is shown graphically in Fig. 4. Presumably (38) can be derived by a more elementary method, but we have been unsuccessful in doing so.

V. EFFECTIVE CONDUCTIVITY

As we mentioned in the Introduction, the problem is to find the function $F(\gamma)$ in (15). The function $F(\gamma)$ contains the information about the long-range Coulomb interaction between all pairs of circles. Obviously, we have to connect the function $F(\gamma)$ with our solution for dipole moment images, (21). But the dipole moment p is related to the polarizability by the relation $p = \beta E_0$, where β is the polarizability. So we first relate $F(\gamma)$ to the pair correction in the polarizability.

Introducing an effective conductivity σ in the observed region containing n circles per unit area, and the mean polarizability of a single inclusion $\overline{\beta}$, we find the Clausius-Mossotti-type result

$$\frac{\sigma - \sigma_0}{\sigma + \sigma_0} = \frac{n\overline{\beta}}{2}, \tag{39}$$

which defines $\overline{\beta}$. The man polarizability $\overline{\beta}$ contains higher-order effects, so we solve (39) for σ/σ_0, and expand it to second order in n,

$$\frac{\sigma}{\sigma_0} = 1 + n\overline{\beta} + \frac{n^2\overline{\beta^2}}{2} + \cdots. \tag{40}$$

Separating the single site and the correction due to pairs in β, we put

$$\overline{\beta} = 2\pi a^2\gamma + \Delta\beta, \tag{41}$$

TABLE I. Taylor series for circular inclusions of conductivity ratio parameter γ.

	Taylor series
Circle	$F(\gamma)=0.666\,67\gamma+0.055\,67\gamma^3+0.013\,17\gamma^5+0.004\,64\gamma^7+0.002\,04\gamma^9$ $+0.001\,04\gamma^{11}+0.000\,58\gamma^{13}+0.000\,35\gamma^{15}+0.000\,22\gamma^{17}+0.000\,15\gamma^{19}$ $+0.000\,10\gamma^{21}+0.000\,07\gamma^{23}+0.000\,05\gamma^{25}+0.000\,04\gamma^{27}+0.000\,03\gamma^{29}$ $+0.000\,02\gamma^{31}+0.000\,02\gamma^{33}+0.000\,02\gamma^{35}+0.000\,01\gamma^{37}+\cdots$

where $\Delta\beta$ is the change in the polarizability due to the presence of other inclusions nearby. Therefore we find (15) in the form

$$\frac{\sigma}{\sigma_0}=1+2\gamma f+2\gamma^2 f^2+n\Delta\beta \tag{42}$$

which is consistent with (16).

The change to the average dipole moment can be written as

$$\overline{P'}=n\int_0^{2\pi}\int_{2a}^{\infty}(P'_{\parallel}\cos^2\theta+P'_{\perp}\sin^2\theta)\,d\theta\,R\,dR, \tag{43}$$

where $P'_{\parallel}$ and $P'_{\perp}$ (and hence $\overline{P'}$) do not contain p_1 (as designated by the primed quantities), but are summed over all the other induced dipoles as in (24) and (25). Terms containing p_1 are already taken in account, in the single-site part of the polarizability [terms proportional to f in (42)].

The series (41) is only conditionally convergent as the leading term involving p_2 is divergent unless the angular integration is done first. Integration over θ gives factor π, and even dipole images cancel out in the integrand, leaving only odd terms doubled. The elimination of the even terms is necessary in order for $F(\gamma)$ to be an odd function of γ, as required by the reciprocity theorem and discussed in Sec. II. It may also be possible to show that the even terms vanish in (41) using methods similar to those of Felderhof, Ford, and Cohen,[14] but this is a lengthy procedure that we have not attempted as we know that the even terms in (41) must integrate to zero using the reciprocity theorem. In three dimensions, the reciprocity theorem cannot be invoked and hence it is necessary to do the analysis surrounding the analogous Eq. (3.35) in Ref. 14.

Recalling the relation between the polarizability and the dipole moment, and Eqs. (24) and (25), we can write

$$\Delta\beta=\frac{\overline{P'}}{E_0}=\frac{2f}{E_0a^2}\int_{2a}^{\infty}(p_3+p_5+p_7+\cdots)R\,dR. \tag{44}$$

The behavior at large R in the integrand in (43) is dominated by the $n=3$ term in the summations in (24) and (25). Thus the asymptotic form of the integrand in (43) varies as R^{-4}, which leads to an absolutely convergent integral in (43) and (44). With the help of (16) the function $F(\gamma)$ is written as

$$F(\gamma)=\frac{2}{\pi E_0a^4}\int_{2a}^{\infty}\frac{(p_3+p_5+p_7+\cdots)}{\gamma^2}R\,dR. \tag{45}$$

Using the hyperbolic function form of the dipole images (21), we have the expression

$$F(\gamma)=16\int_0^{\infty}\sum_{s=1}^{\infty}\gamma^{2s-1}\frac{\sinh^3\alpha\,\cosh\alpha}{\sinh^2(2s+1)\alpha}d\alpha. \tag{46}$$

Finally, (46) can be written in the form

$$F(\gamma)=16(K_1\gamma+K_2\gamma^3+K_3\gamma^5+K_4\gamma^7+\cdots), \tag{47}$$

where K_s is given by

$$K_s=\int_0^{\infty}\frac{\sinh^3\alpha\,\cosh\alpha}{\sinh^2(2s+1)\alpha}d\alpha. \tag{48}$$

Substituting (47) into (15) we have found the expression for the effective conductivity to the second order in the area fraction of the inclusions, f, for any value of γ between 0 and 1:

$$\frac{\sigma}{\sigma_0}=1+2\gamma f+[2\gamma^2+(16K_1\gamma^3+16K_2\gamma^5+16K_3\gamma^7+\cdots)]f^2, \tag{49}$$

where K_s are given by (48). It is useful to simplify the coefficients K_s. First, we transform the integral (48) using the identity

$$\frac{1}{\sinh^2[(2s+1)\alpha]}=\sum_{j=1}^{\infty}\frac{4j}{\exp[2j\alpha(2s+1)]} \tag{50}$$

which can be easily checked.[13] Substituting (50) into (48) we have the following expression for the coefficients K_s:

$$K_s=4\sum_{j=1}^{\infty}j\int\sinh^3\alpha\cosh\alpha\exp[-2j\alpha(2s+1)]d\alpha, \tag{51}$$

which was previously found by Peterson and Hermans,[8] using bipolar coordinates.

Substituting $\omega=\exp[-2j\alpha(2s+1)]$ in (51), carrying out the integration over α,[13] we express the result in terms of the digamma (Ψ) function,

$$K_s=\frac{1}{4(2s+1)^2}\left[\Psi\left(\frac{1}{2s+1}\right)+\Psi\left(\frac{-1}{2s+1}\right)-\Psi\left(\frac{2}{2s+1}\right)-\Psi\left(\frac{-2}{2s+1}\right)\right], \tag{52}$$

which was also found by Peterson and Hermans.[8] The tabulated values of the digamma function were used to construct Table I.

In Fig. 5, we show a plot of $F(\gamma)$, using the Taylor expansion shown in Table I, with enough terms so that convergence was obtained even at $\gamma=1$. This required about 100

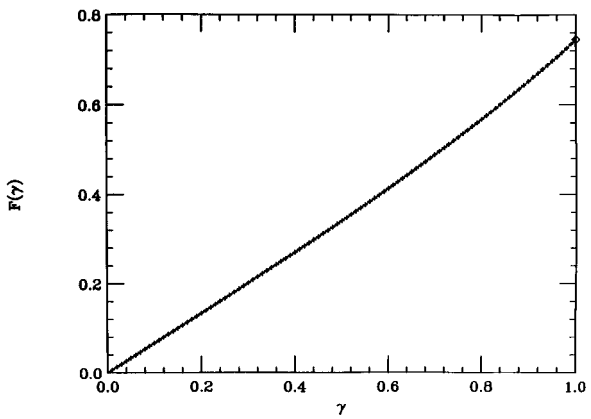

FIG. 5. Interpolation formula (smooth curve) for the function $F(\gamma)$ (crosses). The diamond symbol when $\gamma=1$ is from Eq. (47).

terms to get four-figure accuracy. We have used an approximate interpolation form to fit the result for $F(\gamma)$:

$$F(\gamma)=\frac{2}{3}\frac{\gamma}{(1-b\gamma^2)^c}. \tag{53}$$

The coefficients b and c were chosen to reproduce the result at $\gamma=1$, and the known behavior of $F(\gamma)$ for small γ:

$$F(\gamma)=\tfrac{2}{3}\gamma \quad \text{for small}\,\gamma$$

and (54)

$$F(1)=0.744\,989\,676\ldots.$$

Here the ellipsis following a number denotes that it is known exactly to that number of digits.

Reference 8 contains a numerical error. The last two given coefficients in their formula (67) are 0.0194 and 0.005 05. These should be corrected to 0.0198 . . . and 0.006 97 . . . , respectively.

VI. ANALYTIC CONTINUATION OF THE PAIR TERM

We shall need both the real and imaginary parts of $F(\gamma)$ for the calculation of the spectral function in the next section. The imaginary part can be obtained by analytic continuation. Starting from (46) we rewrite it in slightly different form:

$$F(\gamma)=16\int_0^\infty \sinh^3(\alpha)\cosh(\alpha)\sum_{s=1}^\infty \frac{\gamma^{2s-1}}{\sinh^2[(2s+1)\alpha]}d\alpha. \tag{55}$$

The sum in the integrand

$$A(\gamma)\equiv\sum_{s=1}^\infty \frac{\gamma^{2s-1}}{[e^{\alpha(2s+1)}-e^{-\alpha(2s+1)}]} \tag{56}$$

can be rearranged and expanded in the series

$$A(\gamma)=\sum_{s=1}^\infty \gamma^{2s-1}[e^{-2\alpha(2s+1)}+2e^{-4\alpha(2s+1)} +3e^{-6\alpha(2s+1)}+\cdots]. \tag{57}$$

Introducing the new index $\nu\equiv s-1$ we can transform (57) into

$$A(\gamma)=\gamma\sum_{\nu=0}^\infty\left[\left(\frac{\gamma}{e^{2\alpha}}\right)^{2\nu}e^{-6\alpha}+2\left(\frac{\gamma}{e^{4\alpha}}\right)^{2\nu}e^{-12\alpha} +3\left(\frac{\gamma}{e^{6\alpha}}\right)^{2\nu}e^{-18\alpha}+\cdots\right]. \tag{58}$$

The summation over ν is possible for each term in the square brackets, to give

$$A(\gamma)=\gamma\left[\frac{e^{-6\alpha}}{1-(\gamma/e^{2\alpha})^2}+\frac{2e^{-12\alpha}}{1-(\gamma/e^{4\alpha})^2} +\frac{3e^{-18\alpha}}{1-(\gamma/e^{6\alpha})^2}+\cdots\right], \tag{59}$$

which can be expressed in terms of the variable $x=-1/2\gamma$ as

$$A(x)=-\frac{x}{2}\sum_{m=1}^\infty \frac{me^{-6m\alpha}}{(x)^2-[(e^{-2m\alpha})/2]^2}. \tag{60}$$

We write the function $F(\gamma)$ in (55) in terms of the new variable x:

$$F(x)=-32x\int_0^\infty \sinh^3(\alpha)\cosh(\alpha) \times\left[\sum_{m=1}^\infty \frac{me^{-6m\alpha}}{x^2-[(e^{-2m\alpha})/2]^2}\right]d\alpha \tag{61}$$

or

$$F(x)=-2x\sum_{m=1}^\infty \int_0^{1/2}\frac{(2x')^2[(2x')^{-1/2m}-(2x')^{1/2m}]^3[(2x')^{-1/2m}+(2x')^{1/2m}]}{x^2-x'^2}dx', \tag{62}$$

where we have introduced another new variable, $x'=\frac{1}{2}\exp(-2m\alpha)$. Finally, transforming this expression into partial fraction form, we get after some manipulations

$$F(x)=\int_{-1/2}^{1/2}\frac{\sum_{m=1}^\infty \xi_m(|x'|)}{x-x'}dx' \tag{63}$$

where (writing the dummy variable x' as x)

$$\xi_m(|x|)=4x^2[(2|x|)^{-1/2m}-(2|x|)^{1/2m}]^3 \times[(2|x|)^{-1/2m}+(2|x|)^{1/2m}], \tag{64}$$

and hence, reading from (63), we obtain the imaginary part of $F(x)$ as

$$\mathrm{Im}F(x)=\sum_{m=1}^{\infty}\xi_m(|x|) \tag{65}$$

for $-1/2<x<1/2$. Near $x=0$ there is a cusp,

$$\mathrm{Im}F(x)=1-2|x|+O(|x|^{4/3}), \tag{66}$$

which is caused by the large number of widely separated pairs of circles. We use $\mathrm{Im}F(x)$ to construct the spectral function in the next section.

VII. SPECTRAL REPRESENTATION

It is convenient to change the variables used for the spectral function whose properties were summarized in Sec. I. Using the γ variable defined in (9), instead of the t variable defined in (2), and with $x'=u-\frac{1}{2}$ and $h(x')=g(x'+\frac{1}{2})$, we may rewrite (1) as

$$\frac{\sigma}{\sigma_0}=1+2\gamma\int_{-1/2}^{1/2}\frac{h(x')dx'}{1+2\gamma x'} \tag{67}$$

where

$$\int_{1/2}^{1/2}h(x')dx'=f \tag{68}$$

and

$$\int_{-1/2}^{1/2}x'h(x')dx'=-\frac{f^2}{2}, \tag{69}$$

where f is the concentration (volume fraction) of the phase σ_1 in the host σ_0 [compare with (3) and (4)]. The first moment $\langle x'\rangle$ is now given by

$$\langle x'\rangle=-\frac{f}{2}. \tag{70}$$

For simplicity for the rest of this section, we drop the prime on x. The higher moments of the spectral function $h(x)$ depend on the detailed geometry and are not general like the first moment given by (70). For example, the second moment for the present case is given by

$$\langle x'^2\rangle=2K_1f, \tag{71}$$

where $16K_1$ is the leading term in (46) and from (52) has the numerical value $K_1=1/24$. Hence we have

$$\langle x'^2\rangle=\frac{f}{12}. \tag{72}$$

The spectral function $h(x)$ is formed by taking the imaginary part of σ/σ_0 given by (15) and rearranging so that a self-energy is in the denominator. Such rearrangement can be accomplished formally, as has been done, for example, by Felderhof and Jones[5] and Cichocki and Felderhof.[15] We have been content to write the conductivity in the form (71), which when expanded is equivalent to (42) to second order in the concentration f:

$$\frac{\sigma}{\sigma_0}=\frac{1}{1-2\gamma f/\{1+\gamma f[1-(1/2)F(\gamma)]\}}. \tag{73}$$

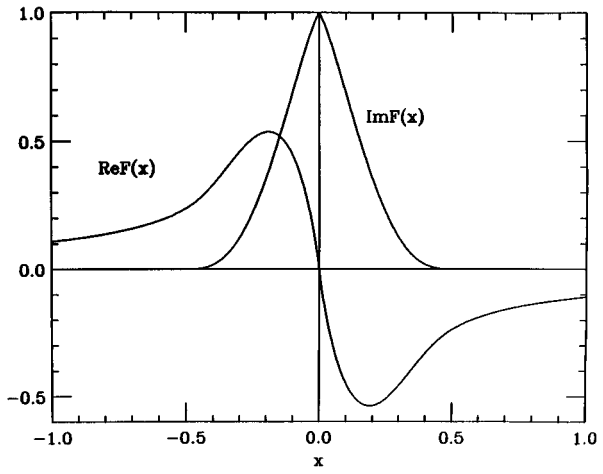

FIG. 6. $\mathrm{Im}F(x)$ and $\mathrm{Re}F(x)$ for circles, with $x=-1/2\gamma$. The real part is obtained from the known imaginary part (64) and (65), using the Kramers-Kronig relation. Note that $\mathrm{Im}F(x)=0$ for $x^2>1/4$.

Taking the imaginary part of (73) (substituting $\gamma=-1/2x$ as before) we have

$$h(x)=\frac{f}{\pi}\frac{[(f/4)\mathrm{Im}F(x)]}{[x+f/2+(f/4)\mathrm{Re}F(x)]^2+[(f/4)\mathrm{Im}F(x)]^2}, \tag{74}$$

where $\mathrm{Re}F(x)$ is the real part of the function F. We obtained it from the known imaginary part in (64) and (65) using the Kramers-Kronig relation. Both $\mathrm{Im}F(x)$ and $\mathrm{Re}F(x)$ are shown in Fig. 6. We plot the spectral function given by (74) for several concentrations f in Fig. 7, using the complete expression (74). Of course, the form (73) is not unique to second order in concentration f. Many other forms can be written down which when expanded will give the conductivity σ correct to order f^2 [see (8)].

We note that Felderhof and Jones[16] also use a continued fraction in their Eq. (3.11) identical to our (74). We prefer the form (73) as it leads to a single smooth spectral function as shown in Fig. 7. The single δ function in the single-inclusion limit is broadened by the interactions between the inclusions at higher concentrations, so that the width is pro-

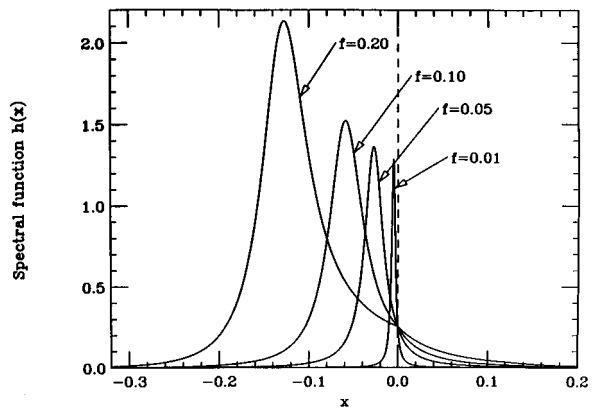

FIG. 7. Spectral function for several values of inclusion area fraction, using (74). $f=0.01,\ 0.05,\ 0.10,\ 0.20$.

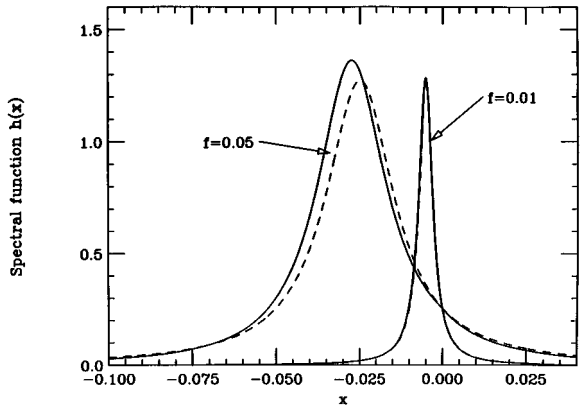

FIG. 8. Lorentzian shape of spectral function $h(x)$ from (75) compared with the exact result (74). The Lorentzian is shown as the dashed line, and the exact result as the solid line, for two concentrations $f=0.05$ and 0.10.

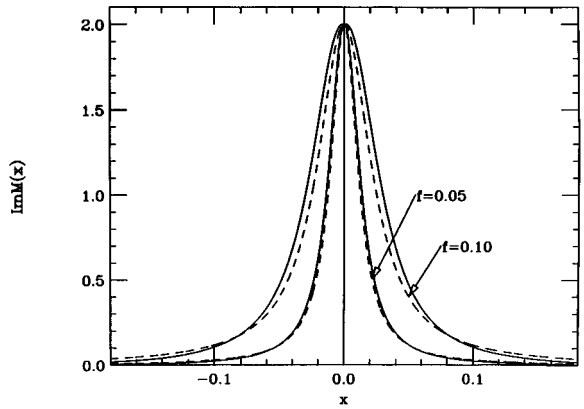

FIG. 9. The function $\mathrm{Im}M(x)$ in the dilute limit. The solid curve is the exact result from (79), and the dashed curve is the Lorentzian approximation (80). Results are shown for two concentrations $f=0.05$ and 0.10.

portional to f as shown in Fig. 7. Similar behavior occurs in the spectral function associated with the vibrations of light point defects in solids.[17] We note that there are no isolated poles in the expression (73) and hence no δ functions in the spectral function, as can be seen from Figs. 7 and 8. This can easily be checked as our spectral functions obey the sum rules (68) and (69). We interpret the spectral function in the low-concentration limit as being analogous to the broadening of single-impurity lines, due to interactions between pairs of light-mass defects in solids.[17] We note that Felderhof and Jones[16] found two isolated δ functions in the spectral function in three dimensions, in addition to a continuous part. These δ functions, we believe, are unphysical and result from the neglect of higher-order multipoles, even at the pair level. Because of the simplifications possible in two dimensions we have been able to sum up all the contributions at the pair level, via the infinite set of dipole images. As a result there are not unphysical δ functions in the spectral function. If we had truncated the expansion (45) after the first few terms, we would have obtained a spectral function with many δ functions, which only form a single continuous function as the series (45) is summed to infinity.

In the dilute limit the spectral function becomes Lorentzian. For small concentrations f, and for small x, using (54) and (66), we can make the approximation $F(x)=i$, i.e., $\mathrm{Re}F(x)\approx 0$ and $\mathrm{Im}F(x)\approx 1$, and the spectral function becomes

$$h(x)=\frac{f}{\pi}\frac{f/4}{(x+f/2)^2+(f/4)^2}. \tag{75}$$

In Fig. 8 we show the spectral function calculated from the full expression (74) and the Lorentzian form (75), for two small concentrations. It can be seen that the differences between these two forms only become apparent at higher values of the area fraction f, where the pair approximation breaks down.

It is easy to find the real part of σ/σ_0 in the dilute limit:

$$\mathrm{Re}\left(\frac{\sigma}{\sigma_0}\right)=1-\frac{2f(2x+f)}{(f/2)^2+(2x+f)^2}. \tag{76}$$

Then, assuming complex x, it is straightforward to show that the complex effective conductivity has the form

$$\frac{\sigma}{\sigma_0}=1-\frac{f}{x+f/2+if/4}, \tag{77}$$

where x is now an arbitrary point in the complex plane. Formula (77) reproduces the correct imaginary and real parts as given by (75) and (76), respectively. Of course, the form (77) is not correct as the single pole is off the real axis, which is not allowed. Also the Lorentzian extends out to $\pm\infty$, which violates the fact that the spectral function is only nonzero between $\pm\frac{1}{2}$. Nevertheless, the Lorentzian form, and hence (77), form a good approximation for small f and x, as shown in Fig. 8.

We also define the function

$$M(\gamma)\equiv\frac{\sigma-\sigma_0}{\sigma+\sigma_0}. \tag{78}$$

It can be shown that the imaginary part of $M(x)$ is given by

$$\mathrm{Im}M(x)=\frac{f}{2}\frac{(f/4)\mathrm{Im}F(x)}{[x+(f/4)\mathrm{Re}F(x)]^2+[(f/4)\mathrm{Im}F(x)]^2}, \tag{79}$$

which in the dilute limit becomes

$$\mathrm{Im}M(x)=\frac{f}{2}\frac{f/4}{x^2+(f/4)^2}. \tag{80}$$

This is both Lorentzian and an even function of x.

In Fig. 9 we contrast plots of the full expression (79) and the Lorentzian form (80) of the function $\mathrm{Im}M(x)$, for two concentrations. Comparing Fig. 9 with Fig. 8 we see that the function $\mathrm{Im}M(x)$ given by (79) keeps its approximate Lorentzian form up to relatively higher concentrations than does the spectral function $h(x)$.

VIII. CONCLUSIONS

We have shown that the spectral function for a sheet containing holes can be calculated correct to second order in the

area fraction of inclusions, f. The result is a truncated Lorentzian that for all practical purposes is a Lorentzian in the range of interest. A knowledge of the spectral function permits the (complex) conductivity σ for any (complex) values of σ_0 and σ_1 to be found, by doing a single integral. This is particularly useful if there is a parameter in the composite that can be varied at fixed geometry. Examples would be the frequency and the temperature.

The calculation in 2D was possible because an exact solution to this problem is available in terms of multiple images. We have managed to do an analytic continuation that has allowed the spectral function to be found, which is finite only over a narrow region at low concentration.

Similar spectral functions can also be used in discrete systems made up of resistors.[18,19] Spectral functions are widely used in physics to study electronic and vibrational excitations. They have proved especially useful in systems containing impurities, where local modes can occur.[17] The weight in the absorption spectrum varies as the defect concentration c and the width is determined by the interaction between defects and varies also as c. The reason for this close analogy between these two somewhat disparate situations is not entirely clear.

ACKNOWLEDGMENTS

We should like to thank P. Leath, G. Milton, and J. Straley for useful discussions, and the Research Excellence Fund of the State of Michigan for financial support.

[1] D. J. Bergman, Phys. Rep. **43**, 377 (1978).
[2] G. W. Milton, J. Appl. Phys. **52**, 5286 (1981).
[3] G. W. Milton, J. Appl. Phys. **52**, 5294 (1981).
[4] K. Golden and G. Papanicolau, Commun. Math. Phys. **90**, 473 (1983).
[5] B. U. Felderhof and R. B. Jones, Z. Phys. B **62**, 215 (1986).
[6] L. D. Landau and E. M. Lifshitz, *Electrodynamics of Continuous Media* (Pergamon, London, 1960), Chap. 9.
[7] M. F. Thorpe, Proc. R. Soc. London Ser. A **437**, 215 (1992).
[8] J. M. Peterson and J. J. Hermans, J. Compos. Mater. **3**, 338 (1969).
[9] K. J. Binns and P. J. Lawrenson, *Electric and Magnetic Field Problems* (Pergamon, Oxford, 1973), pp. 48–53.
[10] J. B. Keller, J. Math. Phys. **5**, 548 (1964).
[11] K. S. Mendelson, J. Appl. Phys. **46**, 917 (1974).
[12] J. Hetherington and M. F. Thorpe, Proc. R. Soc. London Ser. A **438**, 591 (1992).
[13] I. S. Gradshteyn and I. M. Ryzhik, *Table of Integrals and Products* (Academic, New York, 1965).
[14] B. U. Felderhof, G. W. Ford, and E. G. D. Cohen, J. Stat. Phys. **28**, 649 (1982).
[15] B. Cichocki and B. U. Felderhof, J. Stat. Phys. **53**, 499 (1988).
[16] B. U. Felderhof and R. B. Jones, Phys. Rev. B **39**, 5669 (1989).
[17] R. J. Elliott, J. A. Krumhansl, and P. L. Leath, Rev. Mod. Phys. **46**, 465 (1974).
[18] R. M. Foster, Bell Syst. Tech. J. **3**, 651 (1924).
[19] J. P. Straley, J. Phys. C **12**, 2143 (1979).